ARTICLES
PUBLISHED ONLINE: 4 MAY 2015 | DOI: 10.1038/NCHEM.2250
nature chemistry

Adsorption-induced auto-amplification of enantiomeric excess on an achiral surface

Yongju Yun and Andrew J. Gellman*

The homochirality of biomolecules is a signature of life on Earth and has significant implications in, for example, the production of pharmaceutical compounds. It has been suggested that biomolecular homochirality may have arisen from the amplification of a spontaneously formed small enantiomeric excess (e.e.). Many minerals exhibit naturally chiral surfaces and so adsorption has been proposed as one possible mechanism for such an amplification of e.e. Here we show that when gas-phase mixtures of D- and L-aspartic acid are exposed to an achiral Cu(111) surface, a small e.e. in the gas phase, e.e.$_g$, leads to an amplification of the e.e. on the surface, e.e.$_s$, under equilibrium conditions. Adsorption-induced amplification of e.e. does not require a chiral surface. The dependence of e.e.$_s$ on e.e.$_g$ has been modelled successfully using a Langmuir-like adsorption isotherm that incorporates the formation of homochiral adsorbate clusters on the surface.

The homochirality of biomolecules, such as amino acids, sugars, proteins and DNA, is a signature of life on Earth and the mechanistic origins of biomolecular homochirality have been debated for decades[1,2]. It has been suggested that the origin of homochirality in the prebiotic environment was the spontaneous formation of a small e.e. followed by processes that amplify e.e.[3]. Such chiral amplification has been reported in various experiments, including asymmetric autocatalysis, polymerization, crystallization, sublimation and phase transition[4–9]. Chiral amplification phenomena that involve crystalline phases of chiral compounds arise from their tendency to form racemate phases (crystals containing equimolar quantities of both enantiomers) or conglomerate phases (physical mixtures of enantiomerically pure crystals)[10]. Several experiments have demonstrated the impact of chiral surfaces on chiral amplification processes[11–14]. Here we demonstrate that the adsorption-induced auto-amplification of e.e. does not require a chiral surface—it can occur on achiral surfaces. We demonstrate this phenomenon through equilibrium adsorption of non-racemic gas-phase mixtures of D- and L-aspartic acid (Asp, $HO_2C–CH(NH_2)CH_2–CO_2H$) on the achiral Cu(111) surface and suggest a model of homochiral adsorbate clustering that predicts the observed dependence of surface e.e., $\text{e.e.}_s = (\theta_D - \theta_L)/(\theta_D + \theta_L)$, on the gas-phase e.e., $\text{e.e.}_g = (P_D - P_L)/(P_D + P_L)$, where θ_D and P_D are the fractional coverage on the surface and the partial pressure in the gas phase, respectively, of D-Asp (subscript L represents the same for L-Asp).

Symmetry breaking by adsorption on the surfaces of inorganic materials has attracted interest in recent years because naturally chiral minerals, such as quartz, may have played a role in establishing the homochirality of chiral biomolecules[15,16]. Furthermore, enantioselective processes on chiral surfaces of catalytically active materials have potential applications in chiral separations and heterogeneous catalysis[11,17,18]. Hazen *et al.* showed that amino acids, such as Asp, adsorb enantiospecifically on the chiral surfaces of calcite, an achiral mineral that exposes naturally chiral surfaces[15]. Even though metals have achiral bulk structures, they can expose intrinsically chiral surfaces that lack mirror symmetry[19]. It has been shown that chiral adsorbates exhibit enantiospecific orientations, desorption kinetics and reaction energetics on naturally chiral metal surfaces[12,20–26]. Recently, the first unequivocal observation of the enantioselective separation of a racemic mixture on naturally chiral Cu$\{3,1,17\}^{R\&S}$ surfaces was reported; the equilibrium adsorption of racemic D/L-Asp at 460 K results in an e.e.$_s$ of 39 ± 3%[14]. The adsorption of D-Asp is favoured over that of L-Asp on the Cu$\{3,1,17\}^S$ surfaces and vice versa on the Cu$\{3,1,17\}^R$ surfaces.

To create templated chiral surfaces, chiral supramolecular assemblies of organic adsorbates have been formed on metal surfaces[27–30]. Achiral succinic acid forms overlayers on the achiral Cu(110) surface that break the substrate symmetry and, thus, form enantiomorphous domains. A small chiral bias by an enantiomerically pure chiral agent, such as tartaric acid, induces the exclusive formation of one enantiomorph of the succinic acid overlayer[31]. Similarly, Haq *et al.* reported a nonlinear chiral amplification in the supramolecular structure of tartaric acid on Cu(110) induced by a small e.e.$_s$[32]. These examples demonstrate that adsorbate overlayers on achiral surfaces can be made homochiral by a small e.e.$_s$ in the adsorbate composition, a phenomenon known as the 'sergeants and soldiers' effect[31].

Here we report the first observation of auto-amplification of molecular e.e. by equilibrium adsorption of a chiral compound, Asp, on an achiral single crystalline metal surface, Cu(111). In other words, we demonstrate auto-amplification of e.e. in the molecular composition of the adsorbed layer, not just in its supramolecular chiral structure. This work used a ^{13}C-labelling method for the mass spectrometric enantiodiscrimination of adsorbed enantiomers and the determination of e.e.$_s$[14,33,34]. This was coupled with the control of e.e.$_g$ and the ability to establish and quantify equilibrium between gas-phase and adsorbed-phase mixtures of Asp enantiomers. The equilibrium adsorption of gas-phase Asp with e.e.$_g \neq 0$ results in $|\text{e.e.}_s| > |\text{e.e.}_g|$, even though Cu(111) is achiral.

We describe auto-amplification on an achiral surface using a simple Langmuir-like adsorption model. Within this model, chiral auto-amplification is attributed to the homochiral clustering of adsorbates[35–37]. Early observations of the auto-amplification of mixtures of nicotine enantiomers by achiral HPLC columns were also rationalized in terms of the formation of homochiral clusters[35]. Chiral amplification has also been observed during the fragmentation and reformation of octameric serine clusters (Ser$_8$) in the gas

Department of Chemical Engineering, Carnegie Mellon University, Pittsburgh, Pennsylvania 15213, USA. *e-mail: gellman@cmu.edu

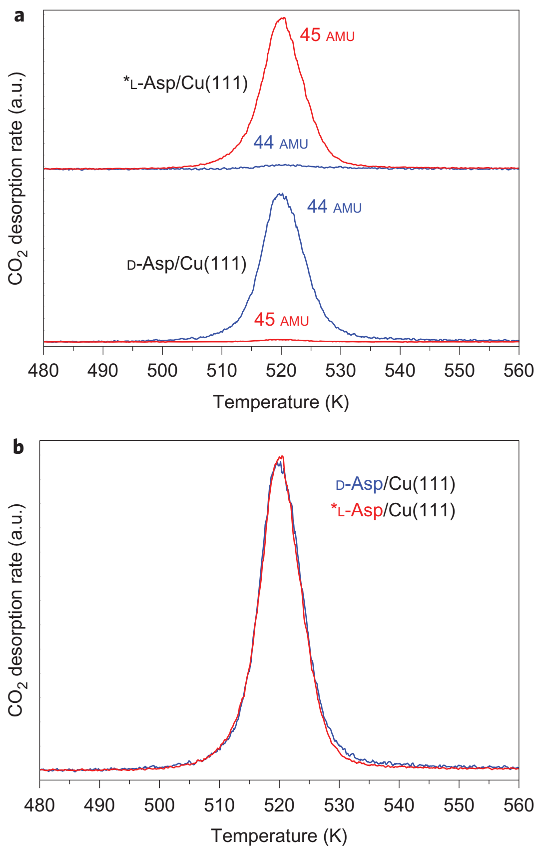

Figure 1 | TPR spectra of D- and *L-Asp on the Cu(111) surface at saturation coverage. a, During heating D- and *L-Asp yield CO_2 (44 AMU) and $^{13}CO_2$ (45 AMU), respectively, and show a clear mass spectrometric enantiodiscrimination of the two enantiomers. Thus, the relative coverages of D- and *L-Asp can be determined from the integrated areas under the CO_2 and $^{13}CO_2$ desorption signals, respectively. **b**, D- and *L-Asp show no measurable ^{13}C-isotope effect on their decomposition kinetics; both decompose at the same temperature, 520 K. a.u., arbitrary units.

phase[9,38]. In general, this type of behaviour arises from the differences in homochiral and heterochiral interactions of chiral molecules and their tendency to form racemate or conglomerate species[10]. Our observation of adsorption-induced auto-amplification on a single crystal surface lends itself to quantitative study, spectroscopic characterization and atomistic modelling, and can provide new insights into enantiomeric amplification processes that may have led to biomolecular homochirality in the prebiotic world. Moreover, adsorption-induced amplification of e.e. must be a fairly general phenomenon and influence enantioselective chemical processes, such as chiral separations and heterogeneous asymmetric catalysis.

Results

This work quantified the equilibria between D/L-Asp mixtures in the gas phase and D/L-Asp mixtures adsorbed on an achiral Cu(111) surface under ultrahigh vacuum conditions. Asp is expected to adsorb on the Cu(111) surface as biaspartate ($^{-}O_2C{-}CH(NH_2)CH_2{-}CO_2^{-}$). On Cu surfaces, with heating biaspartate decomposes into CO_2 (44 AMU), $N{\equiv}CCH_3$ and H_2[14,39]. For the purpose of mass spectrometric enantiodiscrimination of the adsorbed Asp, we used mixtures of isotopically labelled *L-Asp-1,4-$^{13}C_2$ (*L-Asp, $HO_2{}^{13}C{-}CH(NH_2)CH_2{-}{}^{13}CO_2H$) and unlabelled D-Asp. Figure 1a shows the temperature-programmed reaction (TPR) spectra obtained from the decomposition of enantiomerically pure D- and *L-Asp adsorbed on the Cu(111) surface at saturation coverage. As expected, the CO_2 desorption signals are observed at $m/z = 44$ AMU during D-Asp decomposition and $m/z = 45$ AMU during *L-Asp decomposition; CO_2 originates from the carboxylate groups. More importantly, the CO_2 and $^{13}CO_2$ desorption signals can be used to quantify the relative coverages of D- and *L-Asp, θ_D/θ_{*L}. The CO_2 TPR spectra obtained from D- and *L-Asp are indistinguishable (Fig. 1b). Asp exhibits no isotope effect on its decomposition kinetics that might complicate our measurements of adsorption equilibria using D- and *L-Asp[14].

During the initial adsorption of a gas-phase mixture of D- and *L-Asp with the surface at 400 K, the relative coverages of the two enantiomers, θ_D/θ_{*L}, were equal to their relative gas-phase fluxes, P_D/P_{*L}, onto the surface. After saturation of the surface with adsorbed Asp, further exposure with the surface at 460 K resulted in a displacement exchange of the adsorbed Asp by the gas-phase Asp, establishing equilibrium. In this work, the relative equilibrium coverages of D- and *L-Asp on the achiral Cu(111) surface were measured following exposure to gas-phase mixtures with $P_D/P_{*L} = 1/2$, 1 and 2. The partial pressure (flux) ratios were achieved by independently controlling the temperatures of the two glass vials from which the Asp enantiomers were sublimated. The time needed to saturate the surface was ~20 minutes, which indicates that the incident fluxes to the surface correspond to $P \approx 10^{-9}$ torr. After each exposure, the ratio of D/*L-Asp coverages, θ_D/θ_{*L}, on the Cu(111) surface (Fig. 2) was determined from the CO_2 and $^{13}CO_2$ yields measured during TPR spectroscopy.

During exposure to a racemic D/*L-Asp mixture, $P_D/P_{*L} = 1$, the initial coverage ratio was $\theta_D/\theta_{*L} = 1$ because the gas-phase fluxes onto the surface and the sticking coefficients of D- and *L-Asp were identical. After the surface had saturated with adsorbed Asp (<20 minutes), the coverage ratio of D/*L-Asp remained at $\theta_D/\theta_{*L} = 1$ during continued exposure to the racemic D/*L-Asp. This is expected

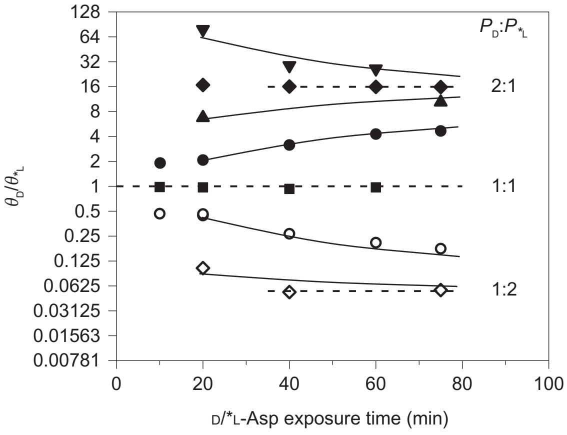

Figure 2 | Asp coverage ratios, θ_D/θ_{*L}, on the achiral Cu(111) surface as a function of exposure time to D/*L-Asp mixtures with partial pressure ratios of P_D/P_{*L} = (1/2), 1 and 2. The uncertainty in each measurement is $\sigma \approx 4\%$. The initial exposure to saturate the surface is at 400 K, whereas further exposure to induced displacement is at 460 K. Exposure to racemic D/*L-Asp in the gas phase results in $\theta_D/\theta_{*L} = 1.0$ (filled squares) for all exposure times, which demonstrates no enantioselectivity. However, exposure to non-racemic D/*L-Asp mixtures of P_D/P_{*L} = (1/2) (open circles) or 2 (filled circles) leads to a decrease or increase of θ_D/θ_{*L}, which reveals enantioselective adsorption on the achiral Cu(111) surface. The data shown with filled inverted triangles, filled diamonds, filled triangles and open diamonds were obtained by starting with θ_D/θ_{*L} = 78, 16, 6.8 and 0.10, respectively. Dashed lines represent equilibrated coverage ratios for the three D/*L-Asp gas-phase mixtures. For the gas-phase D/*L-Asp mixtures with P_D/P_{*L} = (1/2) and 2, the equilibrated coverage ratios on Cu(111) differ by a factor of eight from the partial-pressure ratios in the gas phase.

because neither the D/*L-Asp nor the Cu(111) surface have a net chirality. Exactly the same result was observed on the Cu(100) surface[14]. These constitute control experiments, in that isotope effects arising from our use of ^{13}C-labelled *L-Asp would cause $\theta_{\mathrm{D}}/\theta_{*\mathrm{L}}$ to deviate from unity during exposure to racemic D/*L-Asp. The TPR spectra for D- and *L-Asp shown in Fig. 1b also show no detectable isotope effects.

During the initial exposure of the Cu(111) surface at 400 K to a non-racemic D/*L-Asp mixture with $P_{\mathrm{D}}/P_{*\mathrm{L}} = 2$ the coverage ratio remained $\theta_{\mathrm{D}}/\theta_{*\mathrm{L}} = 2$ until it eached saturation coverage. On chiral Cu$\{3,1,17\}^{R\&S}$ surfaces, D- and *L-Asp have different adsorption energies and displacement leads to an enhancement in the coverage of the enantiomer with the higher adsorption energy during exposure to either racemic or non-racemic mixtures[14]. This would not be expected to occur on the achiral Cu(111) surface. However, continued exposure of the Cu(111) surface at 460 K to the non-racemic mixture with $P_{\mathrm{D}}/P_{*\mathrm{L}} = 2$ resulted in an increase in the coverage ratio to $\theta_{\mathrm{D}}/\theta_{*\mathrm{L}} = 4.7$ (filled circles) (Fig. 2) after exposure for 55 minutes, which demonstrates the enantiopurification of D-Asp by adsorption on an achiral surface. To find the equilibrium value of $\theta_{\mathrm{D}}/\theta_{*\mathrm{L}}$ for the gas-phase flux ratio of $P_{\mathrm{D}}/P_{*\mathrm{L}} = 2$, the surface was first saturated with D/*L-Asp at coverage ratios of $\theta_{\mathrm{D}}/\theta_{*\mathrm{L}} = 6.8$ (filled triangles), 17 (filled diamonds) and 78 (filled inverted triangles) (Fig. 2), and then exposed to the non-racemic mixture with $P_{\mathrm{D}}/P_{*\mathrm{L}} = 2$. Although the values of $\theta_{\mathrm{D}}/\theta_{*\mathrm{L}}$ reached after ~60 minutes of displacement and starting from $\theta_{\mathrm{D}}/\theta_{*\mathrm{L}} = 6.8$ and 78 do not reach the steady-state coverage ratio of $\theta_{\mathrm{D}}/\theta_{*\mathrm{L}} = 16$, they bound this value from above and below. The coverage ratio obtained by starting with $\theta_{\mathrm{D}}/\theta_{*\mathrm{L}} = 17$ tends to a steady-state ratio of $\theta_{\mathrm{D}}/\theta_{*\mathrm{L}} = 16$ after about 20 minutes of displacement. This implies that for $P_{\mathrm{D}}/P_{*\mathrm{L}} = 2$ the equilibrium coverage ratio is $\theta_{\mathrm{D}}/\theta_{*\mathrm{L}} = 16$ and would be reached for any initial coverage ratio, if allowed to equilibrate with the gas-phase Asp for sufficiently long times. This represents an auto-amplification from $\mathrm{e.e.}_{\mathrm{g}} = 34\%(P_{\mathrm{D}}/P_{*\mathrm{L}} = 2.0)$ to $\mathrm{e.e.}_{\mathrm{s}} = 88\%$ $(\theta_{\mathrm{D}}/\theta_{*\mathrm{L}} = 16)$ on the achiral Cu(111) surface.

The initial exposure of the clean Cu(111) surface at 400 K to non-racemic D/*L-Asp with $P_{\mathrm{D}}/P_{*\mathrm{L}} = 0.5$ resulted in a coverage ratio of $\theta_{\mathrm{D}}/\theta_{*\mathrm{L}} = 0.5$ until saturation coverage was reached after 20 minutes. For longer exposure times with the surface at 460 K, displacement resulted in the coverage ratio decreasing to $\theta_{\mathrm{D}}/\theta_{*\mathrm{L}} = 0.18$ (open circles) (Fig. 2), which revealed an amplification of $\mathrm{e.e.}_{\mathrm{s}}$ with the preferential adsorption of *L-Asp. Starting with a coverage ratio of $\theta_{\mathrm{D}}/\theta_{*\mathrm{L}} = 0.10$ (open diamonds) (Fig. 2) and exposing the surface to Asp with $P_{\mathrm{D}}/P_{*\mathrm{L}} = 0.5$ led to a steady-state coverage ratio of $\theta_{\mathrm{D}}/\theta_{*\mathrm{L}} = 0.05$ after 60 minutes of exposure time, roughly equal to the inverse of the equilibrium value of $\theta_{\mathrm{D}}/\theta_{*\mathrm{L}} = 16$ obtained with $P_{\mathrm{D}}/P_{*\mathrm{L}} = 2.0$.

The adsorption-induced amplification of e.e. can best be represented by a plot of $\mathrm{e.e.}_{\mathrm{s}}$ versus $\mathrm{e.e.}_{\mathrm{g}}$. Figure 3 shows the nonlinear relationship between $\mathrm{e.e.}_{\mathrm{s}}$ and $\mathrm{e.e.}_{\mathrm{g}}$ as measured using the method illustrated in Fig. 2. This, too, is a control experiment; if the equilibrium coverage ratios, $\theta_{\mathrm{D}}/\theta_{*\mathrm{L}}$, were observably influenced by ^{13}C-labelling of the *L-Asp, the dependence of $\mathrm{e.e.}_{\mathrm{s}}$ on $\mathrm{e.e.}_{\mathrm{g}}$ would not be symmetric with respect to inversion through the origin. At low values of $\mathrm{e.e.}_{\mathrm{g}}$ the adsorption-induced auto-amplification factor for non-racemic mixtures of D/*L-Asp on the Cu(111) surface was ~8. This remarkable observation is the core result of this work.

Discussion

The adsorption of non-racemic gas-phase mixtures of a chiral compound on an achiral surface can lead to the auto-amplification of e.e. This has important implications for surface chemical processes that are enantioselective, such as adsorption, catalysis and chromatographic separations, and also suggests a novel role that achiral surfaces could have played in the amplification of small chiral biases in the prebiotic world. Our observations raise a number of questions. What is the mechanism of chiral auto-amplification on an achiral surface? Does this mechanism also influence the enantioselective adsorption of chiral compounds on chiral surfaces? What structural characteristics of surfaces and adsorbates govern auto-amplification? This work identified a well-defined model system that can be used to answer some of these questions.

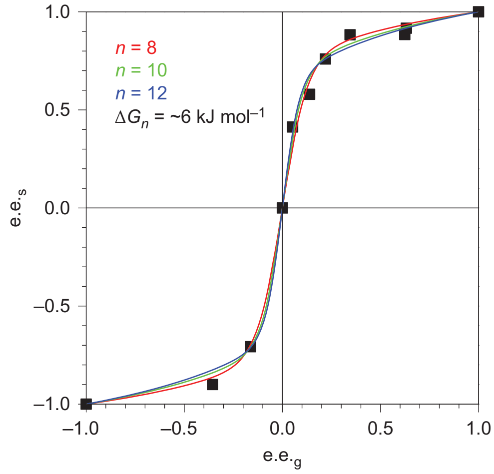

Figure 3 | Relationships between $\mathrm{e.e.}_{\mathrm{g}}$ of the Asp mixtures in the gas phase and the $\mathrm{e.e.}_{\mathrm{s}}$ in the adsorbed phase on an achiral Cu(111) surface under equilibrium adsorption conditions at 460 K. The measurements using Asp mixtures (filled squares) exhibit highly asymmetric adsorption behaviour, which shows that the small $\mathrm{e.e.}_{\mathrm{g}}$ can be auto-amplified to significant values of $\mathrm{e.e.}_{\mathrm{s}}$. The curves are obtained from a Langmuir-like adsorption isotherm that incorporates homochiral cluster formation with cluster sizes of $n = 8$, 10 and 12. The corresponding free energies of cluster formation are $\Delta G_c/n = 6.4$, 5.9 and 5.6 kJ mol^{-1}. The nonlinearity of the isotherms predicted by inclusion of the homochiral cluster formation also predicts the observed auto-amplification of $\mathrm{e.e.}_{\mathrm{s}}$.

The enantioselectivity of Asp adsorption on achiral Cu(111) obviously has a different physical origin than that observed on the chiral Cu$\{3,1,17\}^{R\&S}$ surfaces[14]. On the Cu$\{3,1,17\}^{S}$ surfaces, the equilibrated coverages of D- and *L-Asp can be described by:

$$\frac{\theta_{*\mathrm{L}/R}}{\theta_{\mathrm{D}/R}} = \frac{K_{*\mathrm{L}/R}}{K_{\mathrm{D}/R}}\frac{P_{*\mathrm{L}}}{P_{\mathrm{D}}} = \frac{K_{\mathrm{D}/S}}{K_{*\mathrm{L}/S}}\frac{P_{\mathrm{D}}}{P_{*\mathrm{L}}} = \frac{\theta_{\mathrm{D}/S}}{\theta_{*\mathrm{L}/S}} \qquad (1)$$

where $\theta_{\mathrm{D}/R}$ and $K_{\mathrm{D}/R}$ are the coverage and the equilibrium constant, respectively, for the adsorption of D-Asp on a Cu$\{3,1,17\}^{R}$ surface, $\theta_{*\mathrm{L}/R}$ and $K_{*\mathrm{L}/R}$ are the coverage and the equilibrium constant, respectively, for the adsorption of *L-Asp on a Cu$\{3,1,17\}^{R}$ surface, $\theta_{\mathrm{D}/S}$ and $K_{\mathrm{D}/S}$ are the coverage and the equilibrium constant, respectively, for the adsorption of D-Asp on a Cu$\{3,1,17\}^{S}$ surface and $\theta_{*\mathrm{L}/S}$ and $K_{*\mathrm{L}/S}$ are the coverage and the equilibrium constant, respectively, for the adsorption of *L-Asp on a Cu$\{3,1,17\}^{S}$ surface. The ratios of the equilibrium constants on the two surfaces are $K_{*\mathrm{L}/R}/K_{\mathrm{D}/R} = K_{\mathrm{D}/S}/K_{*\mathrm{L}/S} = 2.2 \pm 0.2$ and are independent of $P_{\mathrm{D}}/P_{*\mathrm{L}}$. Similarly, the coverage ratios of D- and *L-alanine on the Cu$\{3,1,17\}^{R\&S}$ surfaces are proportional to $P_{\mathrm{D}}/P_{*\mathrm{L}}$, although non-enantiospecifically, $K_{*\mathrm{L}/R}/K_{\mathrm{D}/R} = K_{\mathrm{D}/S}/K_{*\mathrm{L}/S} = 1.0$ (ref. 40). This is clearly not the case for the D- and *L-Asp adsorption on Cu(111); even though the surface is achiral, $\theta_{\mathrm{D}}/\theta_{*\mathrm{L}}$ is not proportional to $P_{\mathrm{D}}/P_{*\mathrm{L}}$.

One can imagine several possible mechanisms for the auto-amplification of e.e. on achiral surfaces. Auto-amplification could arise from chiral reconstruction of the surface. There are several examples of chiral adsorbates that reconstruct achiral surfaces and thereby imprint their molecular chirality onto the surface[12,26,41–45].

If imprinting was dominated by the chirality of the majority enantiomer, it could lead to enhanced adsorption of that enantiomer and thus to auto-amplification of e.e.$_s$ with respect to e.e.$_g$. Alternatively, nonlinear competitive adsorption equilibrium processes could lead to auto-amplification.

The Langmuir adsorption isotherm assumes that all the adsorption sites are equivalent and that adsorbates are non-interacting, other than by blocking adsorption on an occupied site. A simple modification to the Langmuir adsorption isotherm can include the effects of adsorbate agglomeration into conglomerate (homochiral) clusters or racemate (heterochiral) clusters. For comparison with the auto-amplification data of Fig. 3, we explored the consequences of a Langmuir-like model that incorporates the formation of homochiral, conglomerate clusters. The simple Langmuir model for competitive adsorption of two enantiomers assumes two equilibrated adsorption processes:

$$\mathrm{D_g} + \square \leftrightarrow \mathrm{D}\square$$

$$\mathrm{L_g} + \square \leftrightarrow \mathrm{L}\square$$

where $\mathrm{D_g}$ is a D-enantiomer in the gas phase, $\square$ is an empty site, $\mathrm{D}\square$ is an adsorbed D-enantiomer and $\mathrm{L}\square$ is an adsorbed L-enantiomer. The equilibrium expressions for the fractional coverages, θ_{D} and θ_{L}, are given by:

$$\theta_{\mathrm{D}} = K_a P_{\mathrm{D}} \delta \qquad (2)$$

$$\theta_{\mathrm{L}} = K_a P_{\mathrm{L}} \delta \qquad (3)$$

where K_a is the adsorption equilibrium constant, which is identical for the D- and L-enantiomers on the achiral surface, and $\delta = (1 - \theta_{\mathrm{D}} - \theta_{\mathrm{L}})$ is the coverage of empty sites. Equations (2) and (3) combined yield well-known expressions for competitive first-order adsorption that cannot predict auto-amplification. The addition of a nonlinear process of homochiral clustering:

$$n(\mathrm{D}\square) \leftrightarrow (\mathrm{D}\square)_n$$

$$n(\mathrm{L}\square) \leftrightarrow (\mathrm{L}\square)_n$$

is described with two additional equilibrium equations:

$$\theta_{\mathrm{D}n} = K_c \theta_{\mathrm{D}}^n \qquad (4)$$

$$\theta_{\mathrm{L}n} = K_c \theta_{\mathrm{L}}^n \qquad (5)$$

where the homochiral clusters contain n molecules and occupy n sites. As the surface is achiral, the equilibrium constants for cluster formation, K_c, are identical for D- and L-enantiomers. The vacancy concentration is now given by:

$$\delta = 1 - \theta_{\mathrm{D}} - \theta_{\mathrm{L}} - n\theta_{\mathrm{D}n} - n\theta_{\mathrm{L}n} \qquad (6)$$

In these terms, the e.e. on the surface is:

$$\mathrm{e.e.}_s = \frac{(\theta_{\mathrm{D}} + n\theta_{\mathrm{D}n}) - (\theta_{\mathrm{L}} + n\theta_{\mathrm{L}n})}{(\theta_{\mathrm{D}} + n\theta_{\mathrm{D}n}) + (\theta_{\mathrm{L}} + n\theta_{\mathrm{L}n})} \qquad (7)$$

These equations can be solved to yield e.e.$_s$ versus e.e.$_g$ for any given choice of the parameters n, K_a, K_c and $P = P_{\mathrm{D}} + P_{\mathrm{L}}$. The positive real roots of the following expression yield the vacancy concentration, δ, versus e.e.$_g$:

$$0 = 1 - (1 + K_a P)\delta - nK_c\left(K_a P/2\right)^n\left((1 + \mathrm{e.e.}_g)^n + (1 - \mathrm{e.e.}_g)^n\right)\delta^n \qquad (8)$$

Given that the experiment dictates that the total coverage of Asp is close to saturation, the vacancy concentrations must have values $\delta \approx 0$. The values of e.e.$_s$ are then given by:

$$\mathrm{e.e.}_s(1 - \delta) = K_a P(\mathrm{e.e.}_g)\delta + nK_c\left(K_a P/2\right)^n \times \left((1 + \mathrm{e.e.}_g)^n - (1 - \mathrm{e.e.}_g)^n\right)\delta^n \qquad (9)$$

For fixed values of n, equations (8) and (9) have been solved to find the values of $K_a P$ and K_c that best fit the data of Fig. 3, and thereby identify the values of n that best reproduce the data.

The data in Fig. 3 show a clear positive deviation of $|\mathrm{e.e.}_s|$ with respect to $|\mathrm{e.e.}_g|$. The homochiral clustering adsorption model predicts an isotherm with $\mathrm{e.e.}_s = \mathrm{e.e.}_g$ for clusters with $n = 1$ (Langmuirian). For $n > 1$ and increasing values of K_c, it predicts an increasing positive deviation of $|\mathrm{e.e.}_s|$ with respect to $|\mathrm{e.e.}_g|$. The three curves shown in Fig. 3 are the solutions to equations (8) and (9) for $n = 8$, 10 and 12, all of which yield fits to the data of similar quality. Fits at lower and higher values of n become increasingly poor. Equilibrium constants, K_c (estimated from the data at 460 K), yield estimates for the free energy of cluster formation of $\Delta G_c/n = 6.0 \pm 0.4$ kJ mol^{-1}, which is quite small and well within the range of dispersion interactions. This simple homochiral clustering model of adsorption is sufficiently nonlinear to predict the auto-amplification observed during exposure of the Cu(111) surface to non-racemic Asp.

Consistent with the model just proposed, there are many observations of amino-acid cluster formation on surfaces[46–52]. Glycine on the Cu(111) surface at 400 K forms trimer rings through hydrogen bonding[51]. A scanning tunnelling microscopy study of alanine on Cu(111) at 473 K showed that alanine forms a hexagonal superstructure with trimer subunits connected by hydrogen bonding[52]. Accompanying density functional theory calculations suggested that the stabilization energies of the alanine trimer relative to three isolated alanine molecules are ~10 kJ mol^{-1} per molecule. Our homochiral clustering model for Asp on Cu(111) provides a comparable value of the cluster stabilization energy. The clustering of amino acids on surfaces is not a novel suggestion; however, that the clusters are homochiral rather than racemic is interesting. During crystallization from the solution or from the gas phase, most amino acids form racemates rather than conglomerates[8]. Our data quite clearly indicate that homochiral interactions, which lead to the formation of conglomerate clusters, dominate over heterochiral interactions, which would lead to the formation of racemate clusters. The formation of racemate clusters would manifest itself by a negative deviation of $|\mathrm{e.e.}_s|$ with respect to $|\mathrm{e.e.}_g|$, opposite to that observed in Fig. 3.

'Self-disproportionation of enantiomers' in the HPLC of enantiomer mixtures on achiral columns results in eluent fractions that differ in e.e. from that of the analyte solution injected onto the column. This is attributed to the inequivalence of homochiral and heterochiral interactions between enantiomers, which leads to the formation of conglomerate or racemic clusters of analyte enantiomers on the stationary phase[35–37]. A related observation is the enantiomeric purification of non-racemic serine in the gas phase by the formation, fragmentation and reformation of gas-phase Ser$_8$ clusters[9,38]. Ser$_8$ clusters form with a high degree of enantiomeric purity and their deposition onto a Au surface allows their collection for the subsequent analysis of e.e. and demonstration of purification over that of the initial Ser mixture. Although enantiopurification was described entirely in terms of gas-phase processes, it is possible that adsorption-induced auto-amplification, as observed for Asp on Cu(111), further enhances the e.e. of Ser$_8$ clusters collected by this process. In addition to these examples of HPLC separations and gas-phase enantiopurification, adsorption-induced auto-amplification must influence the product e.e. of all the enantioselective processes that occur on surfaces. Furthermore, it is important to note that the underlying role of homochiral and heterochiral interactions is just as relevant to processes on chiral surfaces as to those on achiral surfaces.

Conclusions

In this work we report the first example of the auto-amplification of the e.e.$_s$ of a chiral molecule on an achiral metal surface that results from equilibrium adsorption of enantiomeric mixtures with a small e.e.$_g$. Adsorption-induced chiral auto-amplification can be explained by the formation of homochiral clusters on the achiral surface. This chiral amplification mechanism has important implications for the role of inorganic surfaces in the processes that lead to the homochirality of life on Earth. Simple adsorption on an achiral surface can lead to amplification of small enantiomeric excesses that occur under dilute conditions. Furthermore, these auto-amplification processes must impact enantioselective chemical processes, such as adsorption, separations and catalysis, in ways that have not been considered previously.

Methods

The study of the auto-amplification of the e.e. of D- and *L-Asp on the achiral Cu(111) surface was performed in an ultrahigh vacuum system with a base pressure of 2×10^{-10} torr[14,40]. The chamber was equipped with an ion-sputter gun for surface cleaning, low-energy electron diffraction optics to examine the ordering of the clean Cu(111) surface, a homemade evaporator to deposit D-Asp and *L-Asp on the Cu(111) surface and an Extrel mass spectrometer to detect chemical species in the gas phase and those that desorb from the surface during heating. Before each experiment, the surface was cleaned by 1 keV Ar^+ ion sputtering, annealed at 900 K for 500 seconds and then cooled at a controlled rate of -1 K s^{-1} at a pressure of $<1 \times 10^{-9}$ torr. Unlabelled D-Asp (Sigma-Aldrich, 99% chemical purity) and isotopically labelled *L-Asp (Cambridge Isotope Laboratories, 98% chemical purity, 99 atom% 1,4-$^{13}C_2$) were vapour deposited onto the Cu(111) surface by sublimation from two independently heated glass vials. The fluxes of D- and *L-Asp from each vial were controlled by heating the vials to different temperatures in the range 360–390 K. The exposure time was controlled by opening a shutter placed in front of the glass vials. After the exposure to Asp, the Cu sample was resistively heated from 250 K to 670 K at 1 K s^{-1} and the species desorbing from the surface were monitored by the mass spectrometer.

Received 9 January 2015; accepted 25 March 2015;
published online 4 May 2015

References

1. Bonner, W. A. The origin and amplification of biomolecular chirality. *Origins Life Evol. B.* **21,** 59–111 (1991).
2. Bada, J. L. Biomolecules—origins of homochirality. *Nature* **374,** 594–595 (1995).
3. Weissbuch, I., Leiserowitz, L. & Lahav, M. Stochastic 'mirror symmetry breaking' via self-assembly, reactivity and amplification of chirality: relevance to abiotic conditions. *Top. Curr. Chem.* **259,** 123–165 (2005).
4. Soai, K., Shibata, T., Morioka, H. & Choji, K. Asymmetric autocatalysis and amplification of enantiomeric excess of a chiral molecule. *Nature* **378,** 767–768 (1995).
5. Soai, K. *et al.* D- and L-quartz-promoted highly enantioselective synthesis of a chiral organic compound. *J. Am. Chem. Soc.* **121,** 11235–11236 (1999).
6. Green, M. M. *et al.* Majority rules in the co-polymerization of mirror image isomers. *J. Am. Chem. Soc.* **117,** 4181–4182 (1995).
7. Viedma, C. Chiral symmetry breaking during crystallization: complete chiral purity induced by nonlinear autocatalysis and recycling. *Phys. Rev. Lett.* **94,** 065504 (2005).
8. Klussmann, M. *et al.* Thermodynamic control of asymmetric amplification in amino acid catalysis. *Nature* **441,** 621–623 (2006).
9. Perry, R. H., Chunping, W., Nefliu, M. & Cooks, R. G. Serine sublimes with spontaneous chiral amplification. *Chem. Commun.* 1071–1073 (2007).
10. Blackmond, D. G. & Klussmann, M. Spoilt for choice: assessing phase behavior models for the evolution of homochirality. *Chem. Commun.* 3990–3996 (2007).
11. Mallat, T., Orglmeister, E. & Baiker, A. Asymmetric catalysis at chiral metal surfaces. *Chem. Rev.* **107,** 4863–4890 (2007).
12. Gellman, A. J. *et al.* Superenantiospecific chiral surface explosions. *J. Am. Chem. Soc.* **135,** 19208–19214 (2013).
13. Mastai, Y. Enantioselective crystallization on nanochiral surfaces. *Chem. Soc. Rev.* **38,** 772–780 (2009).
14. Yun, Y. & Gellman, A. J. Enantioselective separation on naturally chiral metal surfaces: D,L-aspartic acid on Cu$(3,1,17)^{R\&S}$ surfaces. *Angew. Chem. Int. Ed.* **52,** 3394–3397 (2013).
15. Hazen, R. M., Filley, T. R. & Goodfriend, G. A. Selective adsorption of L- and D-amino acids on calcite: implications for biochemical homochirality. *Proc. Natl Acad. Sci. USA* **98,** 5487–5490 (2001).
16. Hazen, R. M. & Sholl, D. S. Chiral selection on inorganic crystalline surfaces. *Nature Mater.* **2,** 367–374 (2003).
17. Zaera, F. Chiral modification of solid surfaces: a molecular view. *J. Phys. Chem. C* **112,** 16196–16203 (2008).
18. Gellman, A. J. Chiral surfaces: accomplishments and challenges. *ACS Nano* **4,** 5–10 (2010).
19. McFadden, C. F., Cremer, P. S. & Gellman, A. J. Adsorption of chiral alcohols on "chiral" metal surfaces. *Langmuir* **12,** 2483–2487 (1996).
20. Horvath, J. D., Baker, L. & Gellman, A. J. Enantiospecific orientation of *R*-3-methylcyclohexanone on the chiral Cu$\{643\}^{R\&S}$ surfaces. *J. Phys. Chem. C* **112,** 7637–7643 (2008).
21. Gladys, M. J. *et al.* Enantiospecific adsorption of alanine on the chiral Cu{531} surface. *J. Phys. Chem. C* **111,** 8331–8336 (2007).
22. Rampulla, D. M., Francis, A. J., Knight, K. S. & Gellman, A. J. Enantioselective surface chemistry of *R*-2-bromobutane on Cu$(643)^{R\&S}$ and Cu$(531)^{R\&S}$. *J. Phys. Chem. B* **110,** 10411–10420 (2006).
23. Horvath, J. D. & Gellman, A. J. Enantiospecific desorption of *R*- and *S*-propylene oxide from a chiral Cu(643) surface. *J. Am. Chem. Soc.* **123,** 7953–7954 (2001).
24. Horvath, J. D. & Gellman, A. J. Enantiospecific desorption of chiral compounds from chiral Cu(643) and achiral Cu(111) surfaces. *J. Am. Chem. Soc.* **124,** 2384–2392 (2002).
25. Huang, Y. & Gellman, A. J. Enantiospecific adsorption of (*R*)-3-methylcyclohexanone on naturally chiral surfaces vicinal to Cu(110). *Top. Catal.* **54,** 1403–1413 (2011).
26. Cheong, W. Y. & Gellman, A. J. Energetics of chiral imprinting of Cu(100) by lysine. *J. Phys. Chem. C* **115,** 1031–1035 (2011).
27. Lorenzo, M. O., Baddeley, C. J., Muryn, C. & Raval, R. Extended surface chirality from supramolecular assemblies of adsorbed chiral molecules. *Nature* **404,** 376–379 (2000).
28. Ernst, K. H. Supramolecular chirality. *Top. Curr. Chem.* **265,** 209–252 (2006).
29. Barth, J. V. *et al.* Stereochemical effects in supramolecular self-assembly at surfaces: 1D versus 2D enantiomorphic ordering for PVBA and PEBA on Ag (111). *J. Am. Chem. Soc.* **124,** 7991–8000 (2002).
30. Barlow, S. M. & Raval, R. Complex organic molecules at metal surfaces: bonding, organisation and chirality. *Surf. Sci. Rep.* **50,** 201–341 (2003).
31. Parschau, M., Romer, S. & Ernst, K. H. Induction of homochirality in achiral enantiomorphous monolayers. *J. Am. Chem. Soc.* **126,** 15398–15399 (2004).
32. Haq, S., Liu, N., Humblot, V., Jansen, A. P. J. & Raval, R. Drastic symmetry breaking in supramolecular organization of enantiomerically unbalanced monolayers at surfaces. *Nature Chem.* **1,** 409–414 (2009).
33. Nanita, S. C., Takats, Z., Cooks, R. G., Myung, S. & Clemmer, D. E. Chiral enrichment of serine via formation, dissociation, and soft-landing of octameric cluster ions. *J. Am. Soc. Mass Spectrom.* **15,** 1360–1365 (2004).
34. Nanita, S. C. & Cooks, R. G. Serine octamers: cluster formation, reactions, and implications for biomolecule homochirality. *Angew. Chem. Int. Ed.* **45,** 554–569 (2006).
35. Cundy, K. C. & Crooks, P. A. Unexpected phenomenon in the high performance liquid-chromatographic analysis of racemic ^{14}C-labeled nicotine—separation of enantiomers in a totally achiral system. *J. Chromatogr.* **281,** 17–33 (1983).
36. Soloshonok, V. A. Remarkable amplification of the self-disproportionation of enantiomers on achiral-phase chromatography columns. *Angew. Chem. Int. Ed.* **45,** 766–769 (2006).
37. Soloshonok, V. A., Roussel, C., Kitagawa, O. & Sorochinsky, A. E. Self-disproportionation of enantiomers via achiral chromatography: a warning and an extra dimension in optical purifications. *Chem. Soc. Rev.* **41,** 4180–4188 (2012).
38. Fletcher, S. P., Jagt, R. B. C. & Feringa, B. An astrophysically-relevant mechanism for amino acid enantiomer enrichment. *Chem. Commun.* 2578–2580 (2007).
39. Mhatre, B. S. *Super-Enantiospecific Autocatalytic Decomposition of Tartaric Acid and Aspartic Acid on Cu Surfaces* PhD thesis, Carnegie Mellon Univ. (2013).
40. Yun, Y., Wei, D., Sholl, D. S. & Gellman, A. J. Equilibrium adsorption of D- and L-alanine mixtures on naturally chiral Cu$\{3,1,17\}^{R\&S}$ surfaces. *J. Phys. Chem. C* **118,** 14957–14966 (2014).
41. Roth, C., Parschau, M. & Ernst, K. H. Chiral reconstruction of a metal surface by adsorption of racemic malic acid. *ChemPhysChem* **12,** 1572–1577 (2011).
42. Lawton, T. J. *et al.* Long range chiral imprinting of Cu(110) by tartaric acid. *J. Phys. Chem. C* **117,** 22290–22297 (2013).
43. Chen, Q. & Richardson, N. V. Surface facetting induced by adsorbates. *Progr. Surf. Sci.* **73,** 59–77 (2003).
44. Mhatre, B. S. *et al.* A window on surface explosions: tartaric acid on Cu(110). *J. Phys. Chem. C* **117,** 7577–7588 (2013).
45. Zhao, X. Y., Zhao, R. G. & Yang, W. S. Scanning tunneling microscopy investigation of L-lysine adsorbed on Cu(001). *Langmuir* **16,** 9812–9818 (2000).

46. Kuhnle, A., Linderoth, T. R., Hammer, B. & Besenbacher, F. Chiral recognition in dimerization of adsorbed cysteine observed by scanning tunnelling microscopy. *Nature* **415,** 891–893 (2002).
47. Barlow, S. M. *et al.* Supramolecular assembly of strongly chemisorbed size- and shape-defined chiral clusters: *S*- and *R*-alanine on Cu(110). *Langmuir* **20,** 7171–7176 (2004).
48. Schiffrin, A. *et al.* Self-assembly of L-methionine on Cu(111): steering chiral organization by substrate reactivity and thermal activation. *J. Phys. Chem. C* **113,** 12101–12108 (2009).
49. Humblot, V. *et al.* Characterization of two-dimensional chiral self-assemblies L- and D-methionine on Au(111). *Langmuir* **30,** 203–212 (2014).
50. Mahapatra, M. *et al.* Formation of chiral self-assembled structures of amino acids on transition-metal surfaces: alanine on Pd(111). *J. Phys. Chem. C* **118,** 6856–6865 (2014).
51. Zhao, X. Y., Yan, H., Zhao, R. G. & Yang, W. S. Self-assembled structures of glycine on Cu(111). *Langmuir* **19,** 809–813 (2003).
52. Yitamben, E. N. *et al.* Tracking amino acids in chiral quantum corrals. *J. Phys. Chem. C* **117,** 11757–11763 (2013).

Acknowledgements

This work was funded by the US Department of Energy through Grant No. DE-FG02-12ER16330. A.J.G. acknowledges the hospitality of the Fritz-Haber Institute during the writing of this manuscript.

Author contributions

Y.Y. made the initial observation of auto-amplification on a Cu{653} surface. A.J.G. and Y.Y. designed the experiments that demonstrated auto-amplification on the achiral Cu(111) surface. These were performed solely by Y.Y. A.J.G. and Y.Y. analysed the results and prepared the manuscript jointly.

Additional information

Reprints and permissions information is available online at www.nature.com/reprints. Correspondence and requests for materials should be addressed to A.J.G.

Competing financial interests

The authors declare no competing financial interests.